

PCCP

Accepted Manuscript



This is an *Accepted Manuscript*, which has been through the Royal Society of Chemistry peer review process and has been accepted for publication.

Accepted Manuscripts are published online shortly after acceptance, before technical editing, formatting and proof reading. Using this free service, authors can make their results available to the community, in citable form, before we publish the edited article. We will replace this *Accepted Manuscript* with the edited and formatted *Advance Article* as soon as it is available.

You can find more information about *Accepted Manuscripts* in the [Information for Authors](#).

Please note that technical editing may introduce minor changes to the text and/or graphics, which may alter content. The journal's standard [Terms & Conditions](#) and the [Ethical guidelines](#) still apply. In no event shall the Royal Society of Chemistry be held responsible for any errors or omissions in this *Accepted Manuscript* or any consequences arising from the use of any information it contains.

1 **New Particle Formation and Growth from Methanesulfonic Acid, Trimethylamine and**
2 **Water**

3
4 *Haihan Chen, Michael J. Ezell, Kristine D. Arquero, Mychel E. Varner, Matthew L. Dawson, R.*
5 *Benny Gerber, Barbara J. Finlayson-Pitts**

6 Department of Chemistry

7 University of California, Irvine

8 Irvine, CA 92697

9
10 Revision for:

11 Physical Chemistry Chemical Physics

12
13 April 20, 2015

14
15 Corresponding author, Department of Chemistry, University of California, Irvine, CA
16 92697. Email: bjfinlay@uci.edu. Tel: (949) 824-7670; Fax: (949) 824-2420

17
18 Text_MSA+TMA_April20.doc

1 Abstract

2 New particle formation from gas-to-particle conversion represents a dominant source of
3 atmospheric particles and affects radiative forcing, climate and human health. The species
4 involved in new particle formation and the underlying mechanisms remain uncertain. Although
5 sulfuric acid is commonly recognized as driving new particle formation, increasing evidence
6 suggests the involvement of other species. Here we study particle formation and growth from
7 methanesulfonic acid, trimethylamine and water at reaction times from 2.3 to 32 s where
8 particles are 2-10 nm in diameter using a newly designed and tested flow system. The flow
9 system has multiple inlets to facilitate changing the mixing sequence of gaseous precursors. The
10 relative humidity and precursor concentrations, as well as the mixing sequence, are varied to
11 explore their effects on particle formation and growth in order to provide insight into the
12 important mechanistic steps. We show that water is involved in the formation of initial clusters,
13 greatly enhancing their formation as well as growth into detectable size ranges. A kinetics box
14 model is developed that quantitatively reproduces the experimental data under various conditions.
15 Although the proposed scheme is not definitive, it suggests that incorporating such mechanisms
16 into atmospheric models may be feasible in the near future.

17

1 Introduction

2 New particle formation (NPF) from gaseous precursors is an important source of particles in the
3 atmosphere.^{1,2} These newly formed particles can grow and ultimately act as cloud condensation
4 nuclei (CCN), contributing to climate forcing.³⁻⁶ Up to half of global CCN is estimated to
5 originate from NPF.^{5,6} In addition, particles have well-known deleterious impacts on human
6 health^{7,8} and visibility.⁹⁻¹¹ Despite these impacts, the underlying mechanisms and the potential
7 species driving NPF are not well understood. This limits our ability to quantitatively assess the
8 impacts of particles on visibility, human health and climate change as well as to develop
9 effective control strategies.^{1,12}

10 Field measurements have shown that sulfuric acid (H_2SO_4) is a key species for NPF,¹³⁻¹⁵
11 possibly with the involvement of organic compounds.¹⁶⁻¹⁸ The presence of ammonia (NH_3) can
12 stabilize nucleating clusters, and enhance nucleation by orders of magnitude.¹⁹⁻²⁴ However, even
13 taking into account this effect, atmospheric concentrations of H_2SO_4 and NH_3 are often not
14 sufficient to explain nucleation rates in the atmosphere.²³

15 Amines have recently been recognized as additional bases that can participate in NPF.^{22,24-28}
16 Aminium salts from the reaction of acids and amines have been found to be widely present in
17 particles.²⁹⁻³² Amines have a variety of sources, including animal husbandry, biomass burning,
18 industrial and agriculture activities as well as biological processes in the ocean.³³ Release
19 associated with their use in CO_2 capture and storage could become more important as this
20 technology becomes more widely adopted.³³⁻³⁵ Although atmospheric concentrations of amines
21 are typically parts per trillion (ppt), one or more orders of magnitude less than NH_3 , amine
22 concentrations near animal husbandry operations can be up to several parts per billion (ppb).³⁶⁻⁴⁰

1 Amongst over 150 amines that have been identified in the atmosphere,³³ trimethylamine (TMA,
2 $(\text{CH}_3)_3\text{N}$) is one of the most abundant.^{33,40,41}

3 Results from quantum chemical calculations show that amines are much more strongly bound to
4 H_2SO_4 than NH_3 ,²⁵ and laboratory experiments have demonstrated higher efficiencies of amines
5 in particle formation compared to NH_3 .^{22,26,27} In addition, amines have been shown to displace
6 NH_3 in sulfate particles and clusters.⁴²⁻⁴⁵ Based on these results, small particles are more likely
7 to be aminium salts even if ammonium salts are initially formed.

8 While sulfuric acid is often measured in field campaigns and linked to NPF, other sulfur-
9 containing compounds are potentially involved in NPF. For example, methanesulfonic acid
10 (MSA, $\text{CH}_3\text{SO}_3\text{H}$) is commonly detected in particles,^{29,30,46-49} but only a few studies have
11 focused on its potential role in NPF.⁵⁰⁻⁵³ Atmospheric MSA is formed along with SO_2 , the
12 precursor to H_2SO_4 , in the oxidation of organosulfur compounds generated from biological
13 processes, biomass burning and from agricultural, industrial, and domestic activities.⁵⁴⁻⁵⁸ The
14 gas-phase concentration of MSA is typically 10-100% of that of H_2SO_4 in the coastal marine
15 boundary layer.^{59,60} Although MSA was shown to be much less efficient than H_2SO_4 in forming
16 particles with water,^{50-52,61} a recent study from this laboratory found that MSA does form
17 particles with dimethylamine (DMA, $(\text{CH}_3)_2\text{NH}$) and TMA, but only in the presence of water
18 vapor.⁵³ However, this study used a large volume flow system with reaction times from 4.2 min
19 to ~1 hr, so that early stages of particle formation and growth could not be investigated.

20 In the present study, a newly designed and tested borosilicate glass flow system⁶² was applied to
21 investigate particle formation and growth from MSA and TMA at shorter times, from 2.3 to 32
22 seconds. The effect of relative humidity (RH) and precursor concentrations on particle formation

1 and growth is explored. A kinetics scheme for particle formation from MSA, TMA and water
2 that reproduces the experimental data reasonably well is developed based in part on previous
3 quantum chemical calculations of likely early intermediates.⁵³ This approach is sufficiently
4 simple that it could be incorporated into atmospheric models of new particle formation in a
5 relatively straightforward manner.

6 **Experimental**

7 The flow system, described in detail elsewhere,⁶² is shown in Figure 1. Briefly, it is fabricated
8 from borosilicate glass and is designed to cover reaction times from 2.3 to 32 s. The major
9 section of the reactor has a diameter of 7.6 cm and a length of 1.3 m, and is water-jacketed for
10 temperature control. End-caps are mated to each end of the major section and sealed with O-
11 rings. Two perforated hollow glass rings (Fig. 1, ring A and ring B) serve as fixed inlets at the
12 upstream end. Two movable concentric glass tubes are guided by the upstream cap into the
13 reactor, and terminate in two perforated hollow glass “spokes” which serve as the other two
14 inlets (Fig. 1, spokes C and spokes D). A movable stainless steel sampling tube guided by the
15 downstream cap is used to sample particles and gases. The downstream end-cap also has a ½”
16 glass joint to vent the majority of the flow. The reaction time is controlled by changing the
17 distance between the sampling line and the spoke inlets. The distance is then converted to the
18 corresponding reaction time using a previously determined conversion.⁶²

19 The flow reactor was cleaned with Nanopure water (>18.0 MΩ cm; Model 7146; Thermo
20 Scientific), and purged with dry purified air at least overnight. Gas-phase MSA and TMA along
21 with dry/humidified air were introduced into the flow reactor from selected inlets to initiate
22 particle formation and growth. Gas flows were controlled by high precision mass flow

1 controllers (Alicat or MKS), and were regularly calibrated (Gilibrator 2; Sensidyne). Dry
2 compressed air was passed through a purge gas generator (Model 75-62; Parker Balston),
3 carbon/alumina media (Perma Pure, LLC), and a 0.1 μm filter (DIF-N70; Headline Filters) for
4 further purification. Relative humidity was adjusted by diverting part of the dry air flow through
5 a water bubbler filled with Nanopure water. An RH probe (Model HMT338; Vaisala) was
6 placed at the downstream end to monitor RH. Gas-phase MSA was generated by directing dry
7 purified air over liquid MSA (99.0%, Fluka). The concentration of MSA in the flow reactor was
8 controlled by adjusting the flow of purified air over the liquid MSA. It was found necessary to
9 condition the flow reactor with a flow of MSA for two to three days prior to each experiment to
10 passivate the walls with respect to MSA uptake. MSA was measured by passing the gas flow
11 from the MSA trap through a 0.45 μm Durapore filter (Millex-HV) for 5-15 min followed by
12 extraction with 10 mL Nanopure water and analysis using ultra performance liquid
13 chromatography coupled with a tandem mass spectrometer (UPLC-MS/MS, Waters). MSA
14 concentrations in the flow system were then calculated based on the concentration exiting the
15 trap and the total gas flow.

16 Gas-phase TMA (1 ppm in N_2 ; Airgas) was used without further purification. Although certified
17 by the manufacturer, the concentration of TMA was independently measured by collection onto a
18 weak cation exchange resin for 30-60 min followed by extraction with 10 mL 0.1 M oxalic acid
19 (Fluka) and analysis using ion chromatography as previously described.⁴⁰ The measured
20 concentration of TMA, which was generally lower than the value provided by the manufacturer,
21 was used to calculate its concentration in the flow system. This analysis also confirmed that NH_3
22 and other amines were not present at significant levels ($< 0.1\%$ of TMA).

1 All experiments were performed at ambient temperature with a total flow of 17.0 liters per
2 minute (lpm). The mixture of purified air and MSA as well as the mixture of purified air and
3 TMA were separately introduced into the flow system either through the rings or spokes,
4 depending on the experiment. Dry or humidified air was added as a carrier gas and diluent.
5 Particle formation and growth at different reaction times were achieved by changing the position
6 of the sampling line in the flow system. The relative concentrations of MSA, TMA and water
7 vapor and their order of mixing were adjusted to explore their effects on particle formation and
8 growth. Experiments with varied initial concentrations of gaseous precursors, RH and mixing
9 sequence present in this study are tabulated in Table 1.

10 Particle size distributions were monitored using a scanning mobility particle sizer (SMPS)
11 consisting of an electrostatic classifier (Model 3080; TSI), a nano-differential mobility analyzer
12 (Model 3085, TSI), and a butanol-based condensation particle counter (CPC, Model 3776; TSI).
13 The manufacturer specified 50% cut-off size of the SMPS based on sucrose particles is ~ 2.5 nm.
14 While SMPS can detect some particles below 2.5 nm, depending on the composition,⁶³ this
15 portion of the data has high uncertainties and thus was excluded in quantitative analysis. The
16 geometric mean mobility diameters obtained from SMPS are reported as particle diameters.

17 Kinetics schemes for particle formation from MSA, TMA and H₂O were developed and
18 simulated in a box model, in which ordinary differential equations are integrated with the solver,
19 'gsl_odeiv2_step_msbf', provided in the GNU Scientific Library.⁶⁴

20 **Results and Discussion**

21 **Effect of Water on New Particle Formation and Growth.** The effect of water on particle
22 formation and growth was first investigated by mixing 1.8 ppb MSA added through the spokes C

1 with 2.5 ppb TMA added through the spokes D (Exp. 1 and 2 in Table 1). Figure 2 shows
2 particle size distributions as a function of reaction time under dry conditions (Fig. 2a, Exp. 1)
3 and at 48% RH (Fig. 2b, Exp. 2). In the latter case, water vapor was added with air through the
4 upstream inlets of ring A and ring B so that it is present when MSA and TMA react. Further
5 comparisons of particle number concentrations (N_{exp}) and diameters ($D_{p,\text{exp}}$) are shown in Figure
6 3.

7 It is noteworthy that we did not observe particle formation from MSA-H₂O in the absence of
8 TMA (Exp. 3), indicating that there is negligible contamination of ammonia and amines in water.
9 Binary nucleation of MSA-H₂O was reported in previous studies,⁵⁰⁻⁵³ but the nucleation was not
10 as efficient as for H₂SO₄.^{50,61} It is likely that higher MSA levels and longer reaction times than
11 those used in the current study are required to form detectable particles from MSA + H₂O.

12 Although MSA mixed with TMA shows particle formation under both dry and humid conditions,
13 particle formation and growth are much more favorable when water is present. Under dry
14 conditions, particles grow relatively slowly, with $D_{p,\text{exp}}$ increasing from 2.9 to 3.6 nm in 4.9 s, an
15 average growth rate of 0.14 nm s⁻¹. After a short induction time, the particle number
16 concentration increases. Spikes are seen in the size distributions of particles below the SMPS
17 cut-off of 2.5 nm at the shortest times (Fig. 2). Although signal variability precludes
18 quantification at these small sizes, as indicated earlier, the presence of these peaks suggests that
19 there is a pool of small clusters and their growth into detectable sizes is relatively slow under dry
20 conditions. Preliminary experiments using a recently acquired particle size magnifier (PSM,
21 Model A10; Airmodus) which has a cut-off size of ~1.3 nm for ammonium sulfate particles
22 confirms that about 50-70% of particles detected by PSM are smaller than the 2.5 nm cut-off size
23 of SMPS.

1 The presence of water significantly increases both the number concentration and diameter of
2 particles, with particle growth from 4.5 to 7.6 nm in 5.6 s, an average growth rate of 0.55 nm s^{-1} .
3 Even at the shortest experimentally accessible reaction time when particles are relatively small,
4 particles formed under humid conditions are significantly larger than those under dry conditions.
5 The particle number concentration at 48% RH increases in the initial 5 s, and then slowly
6 decreases. However, particles keep growing throughout the experiment. The slow decrease in
7 N_{exp} and increase in $D_{p,\text{exp}}$ after 5 s is due to a combination of the depletion of the gas-phase
8 precursors, coagulation and wall losses. For example, taking a diameter of 8 nm, a particle
9 concentration of $1.7 \times 10^7 \text{ cm}^{-3}$, an assumed density of the condensed phase of 1.3 g cm^{-3} and
10 composition of 1:1:1 MSA:TMA:H₂O, there are 2×10^{10} MSA molecules in the condensed phase
11 per cm^3 of air. Even if the particle has grown primarily through uptake of water to give a particle
12 composition of 1:1:10 MSA:TMA:H₂O, there would be 1×10^{10} MSA molecules per cm^3 of air
13 tied up in condensed phase. Given the difficulty in accurately measuring the concentrations of
14 low volatility species such as MSA, these values are comparable to the initial concentration of
15 MSA (1.8 ppb, $4 \times 10^{10} \text{ cm}^{-3}$), suggesting that a large portion of MSA and TMA is in the
16 condensed phase. Because of the high number concentration and increasing diameters of
17 particles, the remaining gaseous MSA and TMA as well as small clusters can be easily
18 scavenged by existing particles before growing into the detectable size range. In addition,
19 coagulation starts playing a role at particle concentrations $>10^7 \text{ cm}^{-3}$ on the experimental
20 timescale.⁹

21 It is possible that water is not involved in the initial formation of clusters but only grows small
22 particles into diameters $>2.5 \text{ nm}$ that can then be detected. In order to further explore the effect
23 of water, the mixing sequence of MSA, TMA and H₂O in the flow reactor was adjusted (Exp. 4-

1 7). TMA and MSA were separately introduced along with flows of air into the inlets of ring A
2 and ring B at the upstream end of the reactor. The flow from each ring inlet was 7 lpm to make
3 the total flow from the ring inlets 14 lpm. Flows of air through the inlets of spokes C and spokes
4 D were maintained at 2 and 1 lpm, respectively. There is turbulence around the upstream ring
5 inlets that results in significant wall losses of gaseous precursors and particles so that in the
6 configuration of Exp. 4 under dry conditions, the number concentration is smaller than those in
7 Figures 2a and 3a. However, the effect of water can be probed by comparing the results in the
8 presence of water to those under dry conditions where the addition of MSA and TMA remains
9 constant and just the inlet used to add water vapor and its concentration changes.

10 Figure 4 shows the ratios of N_{exp} and $D_{p,\text{exp}}$ collected under humid conditions to those collected
11 under dry conditions at the same reaction time for Exp. 4-7. The addition of water through the
12 spokes C and spokes D corresponding to 18% RH after MSA and TMA from the upstream rings
13 had reacted for 11.6 s (Exp. 5) had no significant effect on the number concentration (Fig. 4a,
14 Exp. 5), but the size of the particles slightly increased (Fig. 4b, Exp. 5). This is consistent with
15 the high hygroscopicity of aminium salts.⁶⁵ In contrast, when water vapor is present
16 simultaneously with MSA and TMA (Exp. 6) the generation of particles in the detectable size
17 range is enhanced. The number concentration and diameter of particles are significantly higher
18 than those formed by adding H₂O after MSA and TMA have reacted. Enhanced particle
19 formation and growth by mixing H₂O simultaneously with MSA and TMA are significant even
20 at 8% RH (Exp. 7). These results show that water is not only involved in particle growth but
21 also plays a central role at the initial stages of particle formation.

22 The fact that adding water vapor after MSA and TMA have reacted for 11.6 s had no effect on
23 the number of detectable particles (Fig. 4a, Exp. 5) suggests that at this point most of the limiting

1 reagent (MSA in this case) is tied up in clusters and particles with TMA, and little gas-phase
2 MSA is available to form particles with TMA and H₂O.

3 **Particle Formation and Growth as a Function of Precursor Concentrations.** The present
4 study enabled measurements of particle formation and growth up to 56% RH, while MSA and
5 TMA concentrations were held constant. The variation of N_{exp} and $D_{p,\text{exp}}$ with reaction time as a
6 function of RH by mixing 1.8 ppb MSA added through the spokes C with 2.0 ppb TMA added
7 through the spokes D is shown in Figure 5 (Exp. 8). Water continues to promote particle
8 formation and growth up to 56% RH, the highest RH used in this study. Significant uncertainties
9 exist at low RH and short reaction times due to the experimental challenges associated with
10 detecting the low numbers of small particles. It is noteworthy that prior to particle formation,
11 there is an induction period of a few seconds, which grows shorter as the RH increases. We
12 hypothesize that this induction period represents the time required for small clusters to grow into
13 detectable-size particles.

14 Formation rates of detectable particles ($J_{\text{exp}, >2.5 \text{ nm}}$) can be estimated using the linear regions of
15 the number concentration-time curves in Figure 5a. The regions that have been used to calculate
16 $J_{\text{exp}, >2.5 \text{ nm}}$ are indicated in Figure S1 in the supplemental information. The values of $J_{\text{exp}, >2.5 \text{ nm}}$
17 are plotted as a function of water vapor concentration in Figure 6. The slopes obtained from
18 three separate experiments (Exp. 8-10) are 1.5 ± 0.2 (2σ), 2.0 ± 0.5 (2σ) and 1.6 ± 0.2 (2σ) with a
19 weighted average of 1.6 ± 0.2 (2σ), suggesting that the overall particle formation rate is
20 approximately 2nd order with respect to water. Water vapor has also been reported to play a role
21 in particle formation from H₂SO₄ and amines.^{22,26,27,66,67} The reaction order of 2 with respect to
22 H₂O does not imply an elementary reaction involving two water molecules nor the number of
23 water molecules in a critical cluster, but rather the involvement of water in the rate-determining

1 step(s).⁶⁸ The 2nd order dependence is captured by the individual steps in the kinetics model as
2 discussed below, and is attributed to the involvement of water in forming the reactive MSA
3 hydrates and/or in subsequent rate-determining step(s).

4 The effects of MSA and TMA on particle formation and growth were further investigated by
5 independently varying the concentration of TMA or MSA at 55% RH as shown in Figures 7 and
6 8. Figure 7 shows N_{exp} and $D_{p,\text{exp}}$ as a function of reaction time while the concentration of TMA
7 increased from 0.7 to 1.1 ppb at a constant MSA of 2.0 ppb (Exp. 11). Figure 8 shows N_{exp} and
8 $D_{p,\text{exp}}$ as a function of reaction time while the concentration of MSA increased from 1.4 to 2.0
9 ppb at a constant TMA of 1.1 ppb (Exp. 12). Both N_{exp} and $D_{p,\text{exp}}$ increase with increasing MSA
10 and/or TMA levels. An induction period before rapid particle formation was observed in all
11 cases but was shorter at higher precursor concentrations.

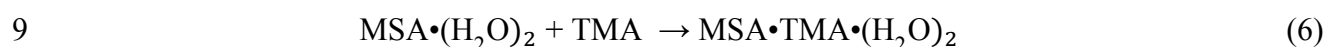
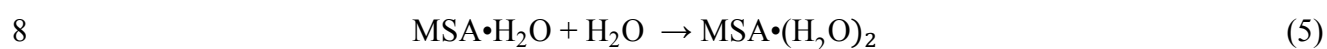
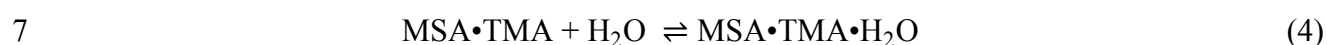
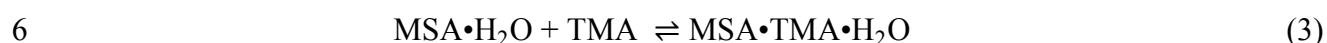
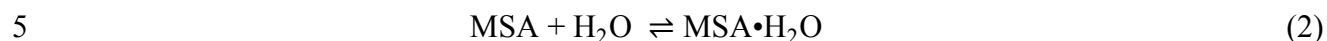
12 **Proposed Kinetics Scheme.** For the formation of particles from sulfuric acid and amines, a
13 "birth-death equations" approach has been developed by others in which the formation and loss
14 of molecular clusters through collisions and evaporation are calculated.^{69,70} The addition of a
15 cluster or molecule to a pre-existing cluster is typically taken to occur at the gas-collision rate.
16 The evaporation rate is obtained from the free energy difference between the product cluster and
17 the reacting species/clusters that formed it, calculated using a quantum chemical approach. This
18 allows for the evaporation of not only monomers but also clusters.⁷¹ Much work has gone into
19 quantum chemical calculations of selected hydrated systems, *i.e.* sulfuric acid with amines or
20 ammonia^{66,67,72-74} and organic acids with ammonia,^{75,76} and comparison with a thermodynamic
21 model has been carried out.⁶⁷ The "birth-death equations" approach has yielded prediction of
22 particle formation rates necessary for analysis and comparison with experimental data in limited
23 cases, such as sulfuric acid with ammonia and dimethylamine.²⁸ Only recently, simulations

1 involving hydrated clusters using their Gibbs free energies in the system of sulfuric acid and
2 dimethylamine were carried out to provide predicted particle formation rates for comparison to
3 observed ones.^{74,77,78} Calculation of free energies for all relevant hydrated clusters up to a
4 reasonable size for incorporation into a “birth-death equation” model is not feasible for the
5 MSA-TMA-H₂O system at the present time. As an alternative, other studies indicate that a
6 kinetics model with adjustable parameters can be used to describe such systems.^{53,79}

7 A simplified kinetics scheme that was previously developed⁵³ was expanded to include
8 individual steps that lead to particles in the MSA-TMA-H₂O system (Fig. 9), and the expanded
9 kinetics scheme was simulated using a box model. A detailed mechanism with 94 species and
10 157 reactions that involves stepwise addition of the gaseous reactants or small clusters is
11 tabulated in Table S1 in the supplemental information. As in the earlier model, the first few
12 steps (reactions (S1-S8) in Table S1) were assumed to be diffusion-controlled in the forward
13 direction, and rate constants were calculated using hard-sphere collision theory.⁵³ Rate constants
14 in the reverse direction were calculated using forward rate constants and ΔG of formation
15 obtained from quantum chemical calculations.⁵³ For the subsequent steps, rate constants were
16 adjusted to fit particle number concentrations obtained from experiments under different
17 conditions. It should be noted that this multistep mechanism and the rate constants are not
18 unique, but simply used to demonstrate that a box model kinetics approach can capture the
19 fundamental behavior of the system. Quantitative treatment of the thermodynamics and kinetics
20 of all of the clusters would be needed to promulgate a definitive mechanism, but is beyond the
21 scope of this work. The basis of the mechanism is the following.

22 First, MSA is known to form hydrates with water.⁵² Figure 10 shows the concentrations and
23 fractional distribution of MSA hydrates at various RH for 2 ppb MSA using published

1 equilibrium constants.⁵² The monohydrate and dihydrate ($n = 1$ or 2) are the two most prominent
2 hydrates at all RH so are included in the model. Both unhydrated and hydrated MSA can react
3 with TMA:⁵³



10 As stated earlier, reactions (1-4) are assumed to be diffusion-controlled in the forward direction,
11 and reversible.^{52,53} No further evaporation of monomer from large clusters or loss of small
12 clusters from large ones as proposed in the H_2SO_4 system^{69,70} was included. Under dry
13 conditions, there are no significant concentrations of hydrates (the presence of some due to trace
14 amounts of water cannot be excluded) and the reaction with TMA forms stable clusters,
15 $\text{MSA} \cdot \text{TMA}$. In a similar vein, H_2SO_4 and DMA have been shown to form an initial
16 $\text{H}_2\text{SO}_4 \cdot \text{DMA}$ cluster which grows by stepwise addition of the acid and base to generate clusters
17 of increasing size with 1:1 stoichiometry.^{28,69,70} Addition of DMA to dimethylammonium salt
18 clusters of MSA was observed to be fastest when there was an excess acid available in the cluster
19 to be neutralized.⁸⁰ This is similar to the case of dry conditions proposed in this study (Pathway
20 I in Fig. 9). In our reaction scheme, the clusters further grow by stepwise addition of MSA and

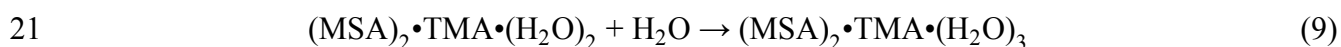
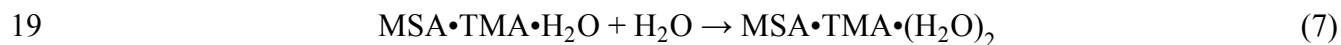
1 TMA or by the addition of MSA•TMA clusters (Pathway I in Fig. 9; Reactions S124-S151 in
2 Table S1) into particles that can be measured by SMPS (>2.5 nm). Loss of MSA•TMA from
3 larger clusters may also occur to significantly slow particle formation and growth under dry
4 conditions. The ion pair formed from MSA and TMA is a particularly stable unit in the MSA-
5 TMA system.⁶⁵ The interaction energy between MSA•TMA units is significant, but not as great
6 as that between ions in the ion pair due to the lack of hydrogen bonding. As discussed in Ortega
7 *et al.*⁷¹ for the sulfuric acid-DMA system, a deep local minimum on the free energy surface can
8 lead to evaporation of clusters that will affect particle formation rates.

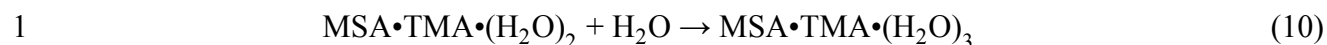
9 As the water vapor concentration increases, hydrated MSA becomes more important so that the
10 initial cluster is now largely MSA•TMA•H₂O. At similar levels of MSA and TMA, the growth
11 of MSA•TMA•H₂O into detectable particles can proceed by adding MSA, hydrated MSA, TMA,
12 MSA•TMA or MSA•TMA•H₂O (Pathway II in Fig. 9; reactions S19-S67 in Table S1). However,
13 with excess MSA (Pathway III in Fig. 9; reactions S68-S102 in Table S1) or TMA (Pathway IV
14 in Fig. 9; reactions S103-S123 in Table S1) present, the excess species can first add to
15 MSA•TMA•H₂O clusters, followed by the stepwise addition of MSA and TMA. As initial
16 clusters grow to a certain size, further growth can proceed by condensation of the excess species.
17 It is assumed that initial concentrations of the gaseous precursors are those in Table 1, but the
18 gases and clusters are lost through a combination of processes that includes loss to the walls and
19 addition to existing particles (Reactions S152-S157 in Table S1). The rate constants for losses of
20 all clusters except MSA, TMA and MSA•H₂O were assumed to be first order, 0.05 s⁻¹. Loss
21 rates for gaseous MSA, TMA, as well as small cluster MSA•H₂O were assumed to be larger
22 since they will diffuse to the walls faster than larger clusters. In each pathway, the growth
23 processes for initial clusters by addition of each type of molecule/cluster are set to have the same

1 rate constant, reducing the number of independent rate constants to 51. For example, reactions
2 (S20), (S26), (S32), (S38), (S44), (S50), (S56) and (S62) in Table S1 showing the growth of
3 clusters by addition of MSA in Pathway II have the same rate constant, $4 \times 10^{-10} \text{ cm}^3 \text{ molecules}^{-1}$
4 s^{-1} . The smallest kinetics model that gives the best fit between laboratory and model predicted
5 number concentrations treats detectable particles as clusters containing ~ 20 molecules for
6 Pathways I and IV, and ~ 30 molecules for Pathways II and III. Clusters that were treated as
7 particles are shown in bold in Table S1.

8 Figure 11 compares the experimental and model results for particle formation in the MSA-TMA-
9 H_2O system under a variety of conditions. Overall, the model calculations agree reasonably well
10 with laboratory results throughout the course of the experiments except the case of excess MSA
11 (Fig. 11d, Exp. 15), in which model calculations reproduce the shape of the time profiles of
12 laboratory results but are approximately 35% lower. Although the proposed kinetics scheme is
13 certainly not unique or definitive, it suggests that particle formation from MSA, TMA and H_2O
14 is a very dynamic and complex process that can, however, be simplified through a series of
15 reactions representing initial cluster formation and growth via addition of MSA, TMA and H_2O ,
16 as well as small clusters.

17 The model also reproduces well the enhancing effect of water in particle formation. Addition of
18 water into initial clusters proceeds through:





2 Reactions (5) and (7) are rate-limiting steps, resulting in an overall second order dependence of
3 particle formation on water.

4 **Atmospheric Implications**

5 Although H_2SO_4 is commonly recognized as the main species driving NPF, increasing evidence
6 from laboratory studies and field measurements has suggested that other species such as MSA
7 also contribute.^{29,30,46-53} Although the concentration of gas-phase MSA is generally lower than
8 that of H_2SO_4 in the atmosphere, the role of MSA in NPF will potentially become more
9 important with the implementation of stricter environmental regulation on SO_2 emissions which
10 lead to H_2SO_4 formation. In addition, it has been predicted that under some conditions, MSA
11 can enhance cluster formation between sulfuric acid and amines.⁸¹

12 Water clearly plays a critical role in particle formation from the reaction of MSA with TMA at
13 the initial stages. Although the specific case described here only involves MSA and TMA, the
14 enhancing effect of water is expected to be applicable to other bases such as ammonia and other
15 amines. This suggests that new particle formation in this system will depend on RH, all other
16 factors being equal. The same may be the case for sulfuric acid reactions with amines.^{22, 26, 27, 66,}
17 ⁶⁷ Although our results suggest that particle formation in this system is quite dynamic and
18 complex, it is still sufficiently straightforward that incorporating such schemes into atmospheric
19 models should be feasible in the near future.

20 **Acknowledgements**

1 The authors are grateful to the National Science Foundation (grant no. 0909227 and 1443140)
2 and the Department of Energy (grant no. ER65208) for funding. We thank Metrohm USA for
3 their support and help in ion chromatography analysis, and Dr. Robert McGraw for helpful
4 discussions.

5

Table 1. The mixing sequence, initial concentrations of gaseous precursors and relative humidity in each experiment

Exp. #	Gas introduced				[MSA] ^a		[TMA] ^a		[H ₂ O]	
	Ring A	Ring B	Spokes C	Spokes D	in ppb	in 10 ¹⁰ cm ⁻³	in ppb	in 10 ¹⁰ cm ⁻³	in %RH	in 10 ¹⁶ cm ⁻³
1	dry air	dry air	MSA	TMA	1.8	4.4	2.5	6.2	<2	<2
2	H ₂ O/air	H ₂ O/air	MSA	TMA	1.8	4.4	2.5	6.2	48	37
3 ^b	H ₂ O/air	H ₂ O/air	MSA	dry air	1.8	4.4	0.0	0.0	50	37
4	TMA	MSA	dry air	dry air	1.7	4.2	5.0	12	<2	<2
5	TMA	MSA	H ₂ O/air	H ₂ O/air	1.7	4.2	5.0	12	18	14
6	TMA + H ₂ O/air	MSA	dry air	dry air	1.7	4.2	5.0	12	19	15
7	TMA + H ₂ O/air	MSA	dry air	dry air	1.7	4.2	5.0	12	8	6
8	H ₂ O/air	H ₂ O/air	MSA	TMA	1.8	4.4	2.0	4.9	7-56	5-42
9	H ₂ O/air	H ₂ O/air	MSA	TMA	3.1	7.6	2.0	4.9	9-59	7-45
10	H ₂ O/air	H ₂ O/air	MSA	TMA	2.7	6.6	1.0	2.5	6-57	5-44
11	H ₂ O/air	H ₂ O/air	MSA	TMA	2.0	4.9	0.7-1.1	1.7-2.7	55	42
12	H ₂ O/air	H ₂ O/air	MSA	TMA	1.4-2.0	3.4-4.9	1.1	2.7	55	42
13	dry air	dry air	MSA	TMA	2.4	5.9	2.0-2.6	4.9-6.4	<2	<2
14	H ₂ O/air	H ₂ O/air	MSA	TMA	0.3	0.7	10-26	25-64	55	42
15	H ₂ O/air	H ₂ O/air	MSA	TMA	14.5	35.7	0.5-0.9	1.2-2.2	55	42

^aSampled from the sources and represent upper limits for the concentrations since some losses may occur between the source and flow tube inlets and in the flow tube itself;

^bNo detectable particles were formed.

References

- 1 1. R. Zhang, A. Khalizov, L. Wang, M. Hu and W. Xu, *Chem. Rev.*, 2011, **112**, 1957-2011.
- 2 2. M. Kulmala, H. Vehkamäki, T. Petäjä, M. Dal Maso, A. Lauri, V. M. Kerminen, W.
- 3 Birmili and P. H. McMurry, *J. Aerosol. Sci.*, 2004, **35**, 143-176.
- 4 3. V.-M. Kerminen, H. Lihavainen, M. Komppula, Y. Viisanen and M. Kulmala, *Geophys.*
- 5 *Res. Lett.*, 2005, **32**, L14803.
- 6 4. D. V. Spracklen, K. S. Carslaw, M. Kulmala, V.-M. Kerminen, S.-L. Sihto, I. Riipinen, J.
- 7 Merikanto, G. W. Mann, M. P. Chipperfield, A. Wiedensohler, W. Birmili and H. Lihavainen,
- 8 *Geophys. Res. Lett.*, 2008, **35**, L06808.
- 9 5. C. Kuang, P. H. McMurry and A. V. McCormick, *Geophys. Res. Lett.*, 2009, **36**, L09822.
- 10 6. J. Merikanto, D. V. Spracklen, G. W. Mann, S. J. Pickering and K. S. Carslaw, *Atmos.*
- 11 *Chem. Phys.*, 2009, **9**, 8601-8616.
- 12 7. C. A. Pope III and D. W. Dockery, *J. Air Waste Manage. Assoc.*, 2006, **56**, 709-742.
- 13 8. M. R. Heal, P. Kumar and R. M. Harrison, *Chem. Soc. Rev.*, 2012, **41**, 6606-6630.
- 14 9. W. C. Hinds, *Aerosol technology: properties, behavior and measurement of airborne*
- 15 *particles*, John Wiley & Sons Inc., New York, 1999.
- 16 10. B. J. Finlayson-Pitts and J. N. Pitts Jr, *Chemistry of the upper and lower atmosphere:*
- 17 *theory, experiments, and applications*, Academic press, San Diego, 2000.
- 18 11. J. H. Seinfeld and S. N. Pandis, *Atmospheric chemistry and physics: from air pollution to*
- 19 *climate change*, John Wiley & Sons, New York, 2006.
- 20 12. T. F. Stocker, Q. Dahe and G.-K. Plattner, *Climate change 2013: the physical science*
- 21 *basis*, Cambridge Univ Press, Cambridge, UK, 2013.
- 22 13. R. J. Weber, G. Chen, D. D. Davis, R. L. Mauldin III, D. J. Tanner, F. L. Eisele, A. D.
- 23 Clarke, D. C. Thornton and A. R. Bandy, *J. Geophys. Res. Atmos.*, 2001, **106**, 24107-24117.
- 24 14. R. J. Weber, J. J. Marti, P. H. McMurry, F. L. Eisele, D. J. Tanner and A. Jefferson,
- 25 *Chem. Eng. Commun.*, 1996, **151**, 53-64.
- 26 15. R. J. Weber, J. J. Marti, P. H. McMurry, F. L. Eisele, D. J. Tanner and A. Jefferson, *J.*
- 27 *Geophys. Res. Atmos.*, 1997, **102**, 4375-4385.
- 28 16. M. Kulmala, J. Kontkanen, H. Junninen, K. Lehtipalo, H. E. Manninen, T. Nieminen, T.
- 29 Petaja, M. Sipila, S. Schobesberger, P. Rantala, A. Franchin, T. Jokinen, E. Jarvinen, M. Aijala, J.
- 30 Kangasluoma, J. Hakala, P. P. Aalto, P. Paasonen, J. Mikkila, J. Vanhanen, J. Aalto, H. Hakola,
- 31 U. Makkonen, T. Ruuskanen, R. L. Mauldin, J. Duplissy, H. Vehkamäki, J. Back, A. Kortelainen,
- 32 I. Riipinen, T. Kurten, M. V. Johnston, J. N. Smith, M. Ehn, T. F. Mentel, K. E. J. Lehtinen, A.
- 33 Laaksonen, V. M. Kerminen and D. R. Worsnop, *Science*, 2013, **339**, 943-946.
- 34 17. M. Ehn, J. A. Thornton, E. Kleist, M. Sipila, H. Junninen, I. Pullinen, M. Springer, F.
- 35 Rubach, R. Tillmann, B. Lee, F. Lopez-Hilfiker, S. Andres, I. H. Acir, M. Rissanen, T. Jokinen,
- 36 S. Schobesberger, J. Kangasluoma, J. Kontkanen, T. Nieminen, T. Kurten, L. B. Nielsen, S.
- 37 Jorgensen, H. G. Kjaergaard, M. Canagaratna, M. Dal Maso, T. Berndt, T. Petaja, A. Wahner, V.
- 38 M. Kerminen, M. Kulmala, D. R. Worsnop, J. Wildt and T. F. Mentel, *Nature*, 2014, **506**, 476-
- 39 479.
- 40 18. F. Riccobono, S. Schobesberger, C. E. Scott, J. Dommen, I. K. Ortega, L. Rondo, J.
- 41 Almeida, A. Amorim, F. Bianchi, M. Breitenlechner, A. David, A. Downard, E. M. Dunne, J.
- 42 Duplissy, S. Ehrhart, R. C. Flagan, A. Franchin, A. Hansel, H. Junninen, M. Kajos, H. Keskinen,
- 43 A. Kupc, A. Kürten, A. N. Kvashin, A. Laaksonen, K. Lehtipalo, V. Makhmutov, S. Mathot, T.
- 44 Nieminen, A. Onnela, T. Petäjä, A. P. Praplan, F. D. Santos, S. Schallhart, J. H. Seinfeld, M.

- 1 Sipilä, D. V. Spracklen, Y. Stozhkov, F. Stratmann, A. Tomé, G. Tsagkogeorgas, P. Vaattovaara,
2 Y. Viisanen, A. Vrtala, P. E. Wagner, E. Weingartner, H. Wex, D. Wimmer, K. S. Carslaw, J.
3 Curtius, N. M. Donahue, J. Kirkby, M. Kulmala, D. R. Worsnop and U. Baltensperger, *Science*,
4 2014, **344**, 717-721.
- 5 19. S. M. Ball, D. R. Hanson, F. L. Eisele and P. H. McMurry, *J. Geophys. Res. Atmos.*, 1999,
6 **104**, 23709-23718.
- 7 20. P. Korhonen, M. Kulmala, A. Laaksonen, Y. Viisanen, R. McGraw and J. H. Seinfeld, *J.*
8 *Geophys. Res. Atmos.*, 1999, **104**, 26349-26353.
- 9 21. D. R. Benson, M. E. Erupe and S.-H. Lee, *Geophys. Res. Lett.*, 2009, **36**, L15818.
- 10 22. T. Berndt, F. Stratmann, M. Sipilä, J. Vanhanen, T. Petäjä, J. Mikkilä, A. Grüner, G.
11 Spindler, R. Lee Mauldin III, J. Curtius, M. Kulmala and J. Heintzenberg, *Atmos. Chem. Phys*,
12 2010, **10**, 7101-7116.
- 13 23. J. Kirkby, J. Curtius, J. Almeida, E. Dunne, J. Duplissy, S. Ehrhart, A. Franchin, S.
14 Gagné, L. Ickes, A. Kürten, A. Kupc, A. Metzger, F. Riccobono, L. Rondo, S. Schobesberger, G.
15 Tsagkogeorgas, D. Wimmer, A. Amorim, F. Bianchi, M. Breitenlechner, A. David, J. Dommen,
16 A. Downard, M. Ehn, R. C. Flagan, S. Haider, A. Hansel, D. Hauser, W. Jud, H. Junninen, F.
17 Kreissl, A. Kvashin, A. Laaksonen, K. Lehtipalo, J. Lima, E. R. Lovejoy, V. Makhmutov, S.
18 Mathot, J. Mikkilä, P. Minginette, S. Mogo, T. Nieminen, A. Onnela, P. Pereira, T. Petäjä, R.
19 Schnitzhofer, J. H. Seinfeld, M. Sipilä, Y. Stozhkov, F. Stratmann, A. Tomé, J. Vanhanen, Y.
20 Viisanen, A. Vrtala, P. E. Wagner, H. Walther, E. Weingartner, H. Wex, P. M. Winkler, K. S.
21 Carslaw, D. R. Worsnop, U. Baltensperger and M. Kulmala, *Nature*, 2011, **476**, 429-433.
- 22 24. J. H. Zollner, W. A. Glasoe, B. Panta, K. K. Carlson, P. H. McMurry and D. R. Hanson,
23 *Atmos. Chem. Phys*, 2012, **12**, 4399-4411.
- 24 25. T. Kurtén, V. Loukonen, H. Vehkamäki and M. Kulmala, *Atmos. Chem. Phys*, 2008, **8**,
25 4095-4103.
- 26 26. M. E. Erupe, A. A. Viggiano and S. H. Lee, *Atmos. Chem. Phys*, 2011, **11**, 4767-4775.
- 27 27. H. Yu, R. McGraw and S.-H. Lee, *Geophys. Res. Lett.*, 2012, **39**, L02807.
- 28 28. J. Almeida, S. Schobesberger, A. Kürten, I. K. Ortega, O. Kupiainen-Määttä, A. P.
29 Praplan, A. Adamov, A. Amorim, F. Bianchi, M. Breitenlechner, A. David, J. Dommen, N. M.
30 Donahue, A. Downard, E. Dunne, J. Duplissy, S. Ehrhart, R. C. Flagan, A. Franchin, R. Guida, J.
31 Hakala, A. Hansel, M. Heinritzi, H. Henschel, T. Jokinen, H. Junninen, M. Kajos, J.
32 Kangasluoma, H. Keskinen, A. Kupc, T. Kurtén, A. N. Kvashin, A. Laaksonen, K. Lehtipalo, M.
33 Leiminger, J. Leppä, V. Loukonen, V. Makhmutov, S. Mathot, M. J. McGrath, T. Nieminen, T.
34 Olenius, A. Onnela, T. Petäjä, F. Riccobono, I. Riipinen, M. Rissanen, L. Rondo, T. Ruuskanen,
35 F. D. Santos, N. Sarnela, S. Schallhart, R. Schnitzhofer, J. H. Seinfeld, M. Simon, M. Sipilä, Y.
36 Stozhkov, F. Stratmann, A. Tomé, J. Tröstl, G. Tsagkogeorgas, P. Vaattovaara, Y. Viisanen, A.
37 Virtanen, A. Vrtala, P. E. Wagner, E. Weingartner, H. Wex, C. Williamson, D. Wimmer, P. Ye,
38 T. Yli-Juuti, K. S. Carslaw, M. Kulmala, J. Curtius, U. Baltensperger, D. R. Worsnop, H.
39 Vehkamäki and J. Kirkby, *Nature*, 2013, **502**, 359-363.
- 40 29. M. C. Facchini, S. Decesari, M. Rinaldi, C. Carbone, E. Finessi, M. Mircea, S. Fuzzi, F.
41 Moretti, E. Tagliavini, D. Ceburnis and C. D. O'Dowd, *Environ. Sci. Technol.*, 2008, **42**, 9116-
42 9121.
- 43 30. A. Sorooshian, L. T. Padró, A. Nenes, G. Feingold, A. McComiskey, S. P. Hersey, H.
44 Gates, H. H. Jonsson, S. D. Miller, G. L. Stephens, R. C. Flagan and J. H. Seinfeld, *Glob.*
45 *Biochem. Cycle*, 2009, **23**, GB4007.
- 46 31. K. A. Pratt, L. E. Hatch and K. A. Prather, *Environ. Sci. Technol.*, 2009, **43**, 5276-5281.

- 1 32. J. N. Smith, K. C. Barsanti, H. R. Friedli, M. Ehn, M. Kulmala, D. R. Collins, J. H.
2 Scheckman, B. J. Williams and P. H. McMurry, *Proc. Natl. Acad. Sci. U. S. A.*, 2010, **107**, 6634-
3 6639.
- 4 33. X. Ge, A. S. Wexler and S. L. Clegg, *Atmos. Environ.*, 2011, **45**, 524-546.
- 5 34. G. T. Rochelle, *Science*, 2009, **325**, 1652-1654.
- 6 35. C. J. Nielsen, H. Herrmann and C. Weller, *Chem. Soc. Rev.*, 2012, **41**, 6684-6704.
- 7 36. T. Fujii and T. Kitai, *Anal. Chem.*, 1987, **59**, 379-382.
- 8 37. N. E. Rabaud, S. E. Ebeler, L. L. Ashbaugh and R. G. Flocchini, *Atmos. Environ.*, 2003,
9 **37**, 933-940.
- 10 38. N. M. Ngwabie, G. W. Schade, T. G. Custer, S. Linke and T. Hinz, *Landbauforschung*
11 *Volkenrode*, 2007, **57**, 273-284.
- 12 39. U. Kuhn, J. Sintermann, C. Spirig, M. Jocher, C. Ammann and A. Neftel, *Geophys. Res.*
13 *Lett.*, 2011, **38**, L16811.
- 14 40. M. L. Dawson, V. Perraud, A. Gomez, K. D. Arquero, M. J. Ezell and B. J. Finlayson-
15 Pitts, *Atmos. Meas. Tech.*, 2014, **7**, 2733-2744.
- 16 41. G. W. Schade and P. J. Crutzen, *J. Atmos. Chem.*, 1995, **22**, 319-346.
- 17 42. B. R. Bzdek, D. P. Ridge and M. V. Johnston, *J. Phys. Chem. A*, 2010, **114**, 11638-11644.
- 18 43. B. R. Bzdek, D. P. Ridge and M. V. Johnston, *Atmos. Chem. Phys*, 2010, **10**, 3495-3503.
- 19 44. Y. Liu, C. Han, C. Liu, J. Ma, Q. Ma and H. He, *Atmos. Chem. Phys*, 2012, **12**, 4855-
20 4865.
- 21 45. C. Qiu, L. Wang, V. Lal, A. F. Khalizov and R. Zhang, *Environ. Sci. Technol.*, 2011, **45**,
22 4748-4755.
- 23 46. J. M. Mäkelä, S. Yli-Koivisto, V. Hiltunen, W. Seidl, E. Swietlicki, K. Teinilä, M.
24 Sillanpää, I. K. Koponen, J. Paatero, K. Rosman and K. Hämeri, *Tellus B*, 2001, **53**, 380-393.
- 25 47. R. J. Hopkins, Y. Desyaterik, A. V. Tivanski, R. A. Zaveri, C. M. Berkowitz, T.
26 Tyliszczak, M. K. Gilles and A. Laskin, *J. Geophys. Res. Atmos.*, 2008, **113**, D04209.
- 27 48. C. J. Gaston, K. A. Pratt, X. Qin and K. A. Prather, *Environ. Sci. Technol.*, 2010, **44**,
28 1566-1572.
- 29 49. S. R. Zorn, F. Drewnick, M. Schott, T. Hoffmann and S. Borrmann, *Atmos. Chem. Phys*,
30 2008, **8**, 4711-4728.
- 31 50. S. M. Kreidenweis and J. H. Seinfeld, *Atmos. Environ.*, 1988, **22**, 283-296.
- 32 51. S. M. Kreidenweis, R. C. Flagan, J. H. Seinfeld and K. Okuyama, *J. Aerosol. Sci.*, 1989,
33 **20**, 585-607.
- 34 52. B. E. Wyslouzil, J. H. Seinfeld, R. C. Flagan and K. Okuyama, *J. Chem. Phys.*, 1991, **94**,
35 6827-6841.
- 36 53. M. L. Dawson, M. E. Varner, V. Perraud, M. J. Ezell, R. B. Gerber and B. J. Finlayson-
37 Pitts, *Proc. Natl. Acad. Sci. U. S. A.*, 2012, **109**, 18719-18724.
- 38 54. T. S. Bates, B. K. Lamb, A. Guenther, J. Dignon and R. E. Stoiber, *J. Atmos. Chem.*,
39 1992, **14**, 315-337.
- 40 55. J. S. VanderGheynst, D. J. Cogan, P. J. DeFelice, J. M. Gossett and L. P. Walker,
41 *Environ. Sci. Technol.*, 1998, **32**, 3713-3718.
- 42 56. P. E. Rosenfeld, C. L. Henry, R. L. Dills and R. B. Harrison, *Water Air Soil Pollut.*, 2001,
43 **127**, 173-191.
- 44 57. S. Meinardi, I. J. Simpson, N. J. Blake, D. R. Blake and F. S. Rowland, *Geophys. Res.*
45 *Lett.*, 2003, **30**, 1454.
- 46 58. I. Barnes, J. Hjorth and N. Mihalopoulos, *Chem. Rev.*, 2006, **106**, 940-975.

- 1 59. F. L. Eisele and D. J. Tanner, *J. Geophys. Res. Atmos.*, 1993, **98**, 9001-9010.
- 2 60. H. Berresheim, T. Elste, H. G. Tremmel, A. G. Allen, H. C. Hansson, K. Rosman, M. Dal
3 Maso, J. M. Mäkelä, M. Kulmala and C. D. O'Dowd, *J. Geophys. Res. Atmos.*, 2002, **107**, 8100.
- 4 61. B. E. Wyslouzil, J. H. Seinfeld, R. C. Flagan and K. Okuyama, *J. Chem. Phys.*, 1991, **94**,
5 6842-6850.
- 6 62. M. J. Ezell, H. Chen, K. D. Arquero and B. J. Finlayson-Pitts, *J. Aerosol. Sci.*, 2014, **78**,
7 30-40.
- 8 63. J. Kangasluoma, C. Kuang, D. Wimmer, M. P. Rissanen, K. Lehtipalo, M. Ehn, D.
9 Worsnop, J. Wang, M. Kulmala and T. Petaja, *Atmos. Meas. Tech.*, 2014, **7**, 689-700.
- 10 64. M. Galassi, *GNU Scientific Library Reference Manual (3rd Ed.)*, ISBN 0954612078,
11 <http://www.gnu.org/software/gsl/>.
- 12 65. M. L. Dawson, M. Varner, V. Perraud, M. J. Ezell, J. Wilson, A. Zelenyuk-Imre, R. B.
13 Gerber and B. J. Finlayson-Pitts, *J. Phys. Chem. C*, 2014, **118**, 29431-29440.
- 14 66. V. Loukonen, T. Kurten, I. K. Ortega, H. Vehkamäki, A. A. H. Padua, K. Sellegri and M.
15 Kulmala, *Atmos. Chem. Phys.*, 2010, **10**, 4961-4974.
- 16 67. H. Henschel, J. C. A. Navarro, T. Yli-Juuti, O. Kupiainen-Määttä, T. Olenius, I. K.
17 Ortega, S. L. Clegg, T. Kurtén, I. Riipinen and H. Vehkamäki, *J. Phys. Chem. A*, 2014, **118**,
18 2599-2611.
- 19 68. O. Kupiainen-Määttä, T. Olenius, H. Korhonen, J. Malila, M. Dal Maso, K. Lehtinen and
20 H. Vehkamäki, *J. Aerosol. Sci.*, 2014.
- 21 69. M. J. McGrath, T. Olenius, I. K. Ortega, V. Loukonen, P. Paasonen, T. Kurtén, M.
22 Kulmala and H. Vehkamäki, *Atmos. Chem. Phys.*, 2012, **12**, 2345-2355.
- 23 70. T. Olenius, O. Kupiainen-Määttä, I. K. Ortega, T. Kurtén and H. Vehkamäki, *J. Chem.*
24 *Phys.*, 2013, **139**, 084312.
- 25 71. I. K. Ortega, O. Kupiainen, T. Kurten, T. Olenius, O. Wilkman, M. J. McGrath, V.
26 Loukonen and H. Vehkamäki, *Atmos. Chem. Phys.*, 2012, **12**, 225-235.
- 27 72. D. J. Bustos, B. Temelso and G. C. Shields, *J. Phys. Chem. A*, 2014, **118**, 7430-7441.
- 28 73. J. W. DePalma, D. J. Doren and M. V. Johnston, *J. Phys. Chem. A*, 2014, **118**, 5464-5473.
- 29 74. A. B. Nadykto, J. Herb, F. Yu and Y. Xu, *Chem. Phys. Lett.*, 2014, **609**, 42-49.
- 30 75. K. H. Weber, Q. Liu and F.-M. Tao, *J. Phys. Chem. A*, 2014, **118**, 1451-1468.
- 31 76. W. Xu and R. Zhang, *J. Chem. Phys.*, 2013, **139**, 064312.
- 32 77. O. Kupiainen-Määttä, H. Henschel, T. Kurtén, V. Loukonen, T. Olenius, P. Paasonen and
33 H. Vehkamäki, *Chem. Phys. Lett.*, 2015, **624**, 107-110.
- 34 78. A. B. Nadykto, J. Herb, F. Yu, E. S. Nazarenko and Y. Xu, *Chem. Phys. Lett.*, 2015, **624**,
35 111-118.
- 36 79. M. Chen, M. Titcombe, J. Jiang, C. Jen, C. Kuang, M. L. Fischer, F. L. Eisele, J. I.
37 Siepmann, D. R. Hanson, J. Zhao and P. H. McMurry, *Proc. Natl. Acad. Sci. U. S. A.*, 2012, **109**,
38 18713-18718.
- 39 80. B. R. Bzdek, D. P. Ridge and M. V. Johnston, *J. Geophys. Res. Atmos.*, 2011, **116**,
40 D03301.
- 41 81. N. Bork, J. Elm, T. Olenius and H. Vehkamäki, *Atmos. Chem. Phys.*, 2014, **14**, 12023-
42 12030.
- 43